ELSEVIER

Journal of Nuclear Materials 320 (2003) 214–222

journal of nuclear materials

www.elsevier.com/locate/jnucmat

Gas-driven hydrogen permeation in the surface-limited regime

A. Pisarev [a,*,1], V. Shestakov [b], R. Hayakawa [a], Y. Hatano [a], K. Watanabe [a]

[a] *Hydrogen Isotope Research Center, Toyama University, Toyama 930-8555, Japan*
[b] *The State University of Kazakhstan, Almaty 480100, Kazakhstan*

Received 12 December 2001; accepted 23 February 2003

Abstract

Gas-driven permeation of hydrogen through metal membranes in the surface-limited regime (SLR) is analyzed. An analytical solution for the concentration and permeation flux as a function of time is given for permeation through the asymmetric membrane having different conditions on the inlet and outlet sides. The features of the steady state and transient permeation are discussed. Comparison of calculations with an experiment on deuterium permeation through vanadium, which is available from literature, is performed. It has been demonstrated that the parameters, extracted from the measurements of the permeation rate in SLR are very uncertain. Even the calculations with opposite asymmetries can be equally well adjusted to the experiment. Non-zero initial conditions in SLR experiments are additional source of uncertainty. Measurements of the accumulation in a closed volume instead of the permeation rate can seriously mislead in the interpretation of the experiment. Complementary experiments on permeation in two opposite directions and measurements of permeation decay could increase the reliability of the data obtained.

PACS: 66.30.−h; 68.47.−b; 82.20.Pm

1. Introduction

Gas-driven permeation is a method, which is widely used for investigations of hydrogen behavior in solids. This behavior is determined at least by bulk diffusion and surface effects.

Initially, permeation was considered only as a diffusion-limited process. Richardson et al. were the first who proposed in 1904 [1] the model of steady state permeation of hydrogen through the membrane that was based on the suggestion that particles moved in the field of the concentration gradient according to Fick's law. The concentration near the inlet surface was set as a constant proportional to the square root of the gas pressure, while the concentration on the back side was set equal to zero. Daynes in 1920 [2] obtained the equation for dynamics of permeation after an abrupt pressure application on the inlet side of a membrane.

Surface effects were out of consideration in those times in application to permeation experiments, but they were considered in application to adsorption and absorption experiments. Particularly, Wagner in 1932 [3] wrote a mass balance equation for accumulation of hydrogen in palladium in the surface-limited regime (SLR). It was accepted that absorption of hydrogen in metal is due to dissociation and desorption is due to recombination. The equation was solved, and the result was the time dependence of hydrogen concentration in metal.

Wang seems to have been the first who presented in 1936 [4] the permeation model, which incorporated surface effects. Along with diffusion, he considered hydrogen transfer processes through the inlet and outlet surfaces. Those were dissociative chemisorption on the surface, recombinative desorption from the surface, and

* Corresponding author. Tel.: +7-095 323 9325; fax: +7-095 324 7024.
E-mail address: pisarev@plasma.mephi.ru (A. Pisarev).
[1] Present address: Moscow Engineering and Physics Institute, Moscow 115409, Russia.

0022-3115/03/$ - see front matter
doi:10.1016/S0022-3115(03)00110-7

reversible transitions between under-surface bulk sites and on-surface chemisorption sites.

Livshits in 1977 [5] used the scheme similar to that of Wang and first predicted that asymmetry of surface conditions on the inlet and outlet sides can strongly affect permeation.

Ali-Khan et al. in 1978 [6] simplified Wang's model and wrote the desorption rate to be proportional to the square of the bulk concentration multiplied by an effective recombination coefficient. A general implicit expression for the steady state permeation rate was obtained, which can be applied in any regime of permeation: diffusion-limited, surface-limited, and intermediate. Only the case of identical surfaces (symmetric membrane) was considered.

Waelbroeck et al. in 1984 [7] extended the model of surface-limited absorption [3] onto the case of surface-limited permeation and wrote a formula for the permeation rate as a function of time ('transient permeation') in SLR for the case of the asymmetric membrane. The authors analyzed influence of the recombination coefficients on the inlet and outlet sides, made the conclusion that permeation can be limited by processes either on the inlet or outlet surfaces, analyzed permeation in two opposite directions, and paid attention to possible influence of non-zero initial concentration.

The present paper is based on the approach developed by Waelbroeck et al. [7]. We will obtain a new formula for the dynamics of the permeation and find the approximation formulas for the concentration, permeation rate, and characteristic time in the cases of absorption-limited and recombination-limited regimes of permeation. Then we will demonstrate some effects that follow from analytical formulas. Finally, we will compare the model calculations with an experiment on permeation of hydrogen through vanadium, and discuss problems in extraction of the recombination coefficients and solubility from experiments with asymmetric membranes.

2. SLR model

The SLR is characterized by a relatively high diffusion rate. Therefore, the concentration profile can be considered to be flat. The concentration evolution in time $C(t)$ [at m^{-3}] is determined by three fluxes [at m^{-2} s^{-1}]: (1) $i_a = 2K_a p$ is the absorption flux (particles, which enter the membrane from the inlet side); (2) $j_r = K_1 C^2$ is the re-emission flux (particles, which desorbed from the inlet side); and (3) $j = j_p = K_2 C^2$ is the permeation flux (particles, which desorbed from the outlet side):

$$L\,\mathrm{d}C/\mathrm{d}t = i_a - (j_r + j_p) = 2K_a p - (K_1 + K_2)C^2. \tag{1}$$

Here L is the thickness of the membrane [m], p the gas pressure [Pa], K_a the absorption coefficient [at m^{-2} s^{-1} Pa^{-1}] on the inlet side, and K_1 and K_2 the recombination coefficients [m^4 s^{-1} at^{-1}] on the inlet and the outlet sides of the membrane, respectively. This equation is equivalent to that used in [7].

Separating the variables in Eq. (1) and integrating, one can obtain

$$L\int \mathrm{d}C[2K_a p - (K_1 + K_2)C^2]^{-1} = \int \mathrm{d}t. \tag{2}$$

The integral on the left can be reduced to the standard integral, which gives

$$\operatorname{arctanh}(C/C_m) - \operatorname{arctanh}(C_0/C_m) = t/\tau, \tag{3}$$

from which

$$C = C_m \tanh[t/\tau + \operatorname{arctanh}(C_0/C_m)] \tag{4}$$

and

$$j = j_m \tanh^2[t/\tau + \operatorname{arctanh}(C_0/C_m)]. \tag{5}$$

Here $C(t=0) = C_0$ is the initial concentration, C_m the concentration in the steady state, j_m the steady state permeation rate, and τ the characteristic time given by the following expressions:

$$C_m = (2K_a p)^{1/2}(K_1 + K_2)^{-1/2}, \tag{6}$$

$$j_m = K_2 C_m^2 = (2K_a p)K_2(K_1 + K_2)^{-1}, \tag{7}$$

$$\begin{aligned}\tau &= L[2K_a p(K_1 + K_2)]^{-1/2} = LC_m^{-1}(K_1 + K_2)^{-1} \\ &= C_m L/2K_a p.\end{aligned} \tag{8}$$

The characteristic time τ has the simple physical meaning, which follows from Eq. (8): this is the time necessary to build up the concentration from zero to the final value C_m at the incoming flux $2K_a p$ if there is no hydrogen release from the membrane.

The absorption coefficient and the recombination coefficient on the inlet side are mutually connected by the condition superimposed by equilibrium between gas and solid ($i_a = j_r$) in experiments on absorption, where $j_p = 0$:

$$2K_a p = K_1 C_S^2 = K_1 S^2 p. \tag{9}$$

Here $C_S = Sp^{1/2}$ is the saturation, or Sieverts', concentration in a sample with the solubility S, which is embedded in gas of the pressure p.

Having this correlation, one can rewrite the expressions for C_m, τ, and j_m in the form convenient for analysis of the asymmetry influence:

$$C_m = Sp^{1/2}(K_1)^{1/2}(K_1 + K_2)^{-1/2}, \tag{10}$$

$$\tau = LS^{-1}p^{-1/2}[K_1(K_1 + K_2)]^{-1/2}, \quad (11)$$

$$j_m = S^2 pK_1K_2(K_1 + K_2)^{-1}. \quad (12)$$

The concentrations and the permeation flux normalized to the respective maximum values C_m and $j_m = K_2C_m^2$ are universal functions of the dimensionless time t/τ, as it follows from Eqs. (4) and (5). Fig. 1 shows these dependences for three values of the initial concentration.

The initial mass balance Eq. (1), which we used for writing Eq. (5), is the same as that used in [7]. But the formula obtained by Waelbroeck et al. in [7] rewritten in our denotations is different:

$$j = j_m[\tanh(t/\tau) + C_0/C_m]^2/[C_0/C_m \tanh(t/\tau) + 1]^2. \quad (13)$$

Eqs. (5) and (13) are compared in Fig. 1. One can see that they give the same result.

It was mentioned in [7] that it is usually wrong to suggest that the initial concentration is zero for metals, which give SLR of permeation, because the outgasing rate is very low between the permeation runs. Fig. 1 shows the comparison of the dynamics of permeation in the cases $C_0 = 0$ and $C_0 \neq 0$. One can see that they are principally different in the beginning of the permeation run: in the first case, the permeation rate increases as the square of time while in the second case it increases approximately linearly with time. The squared dependence of the initial permeation rate in the case of the zero initial concentration follows from Eq. (1): if to set $C = 0$ in the right part of the equation, we obtain a linear $C(t)$ dependence, which gives a squared $j(t)$ dependence.

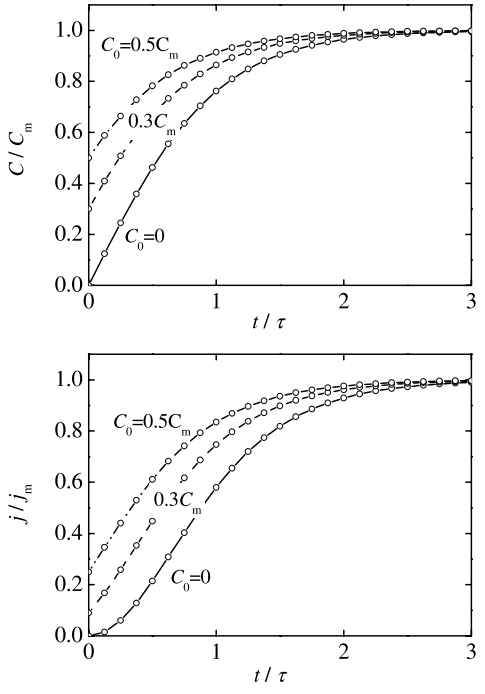

Fig. 1. The concentration (expressed in units of the maximum concentration C_m) and the permeation rate of particles (in units of the maximum permeation rate j_m) as functions of time (expressed in units of the characteristic time τ) for three values of the initial concentration. Lines – the formulas of the present work, dots – those from Waelbroeck et al. [7].

Experiments are often performed in the so-called accumulation mode, where the permeating gas is collected in a closed vacuum chamber. The number of permeated particles can be found by integration of the permeation flux over the time. Fig. 2 demonstrates the universal accumulation curves obtained at two values of the initial concentration. The accumulation is normalized to the product $j_m\tau$. At large times, $Q(t)$ curve can be interpolated by a straight line. The intersection of this line with the t axis gives the lag time of permeation, which depends on the initial concentration. One must mention here that the lag time and the characteristic time τ are not the same values. If $C_0 = 0$, the lag time equals τ, and the straight line approximation intersects the time axis at $\tau = 1$ in Fig. 2. If $C_0 \neq 0$, the lag time is less than τ. This effect can entail serious problems when interpreting the experimental data. Firstly, it brings uncertainty in determination of the recombination coefficients and solubility. Secondly, if the initial concentration becomes rather high, the lag time can decrease down to the values typical for the diffusion-limited regime (DLR) of permeation. This can mislead in the interpretation of the experiment.

The characteristic times in SLR and in DLR have different dependences on the sample thickness and the driving gas pressure. The characteristic time is proportional to the thickness in SLR and to the square of the thickness in DLR. Besides, it is pressure independent in DLR but it is inversely proportional to the square root

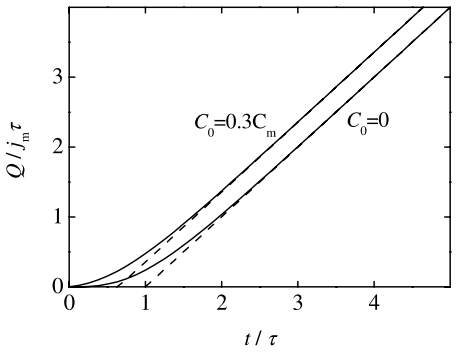

Fig. 2. The number of permeated particles (in units of $j_m\tau$) as a function of time (in units of τ) for two values of the initial concentration.

of the pressure in SLR. The latter dependence (along with the often used $j_m(p)$ dependence) can serve for verification of the regime of permeation in the experiment.

3. Two modes of SLR

It has been mentioned in [7] that depending on the relation between K_1 and K_2, permeation is limited either by absorption on the inlet side if $K_1 \ll K_2$ or by recombinative desorption on the outlet side if $K_2 \ll K_1$. That is, SLR has two modes: the absorption-limited regime (ALR) and the recombination-limited regime (RLR). If to introduce the asymmetry parameter $\gamma = K_2/K_1$, one can say that $\gamma \gg 1$ is the case of ALR and $\gamma \ll 1$ is the case of RLR.

The formulas for the permeation rate, concentration, and characteristic time can be simplified in the limits of ALR and RLR. Table 1 gives the formulas for C_m, τ, and j_m for the general case, for the case of a symmetric membrane, and for the cases of ALR and RLR. The parameters are normalized to some coefficients to demonstrate influence on K_1 and K_2 only. Additional function included in Table 1 is j_m/i_a which is the part of absorbed particles that is not re-emitted from the inlet side but desorbed from the outlet side after permeating through the membrane. Let us remind that $i_a = 2K_a p = K_1 C_S^2$.

4. Steady state features

In the case of symmetric membranes ($K_1 = K_2 = K$), the steady state concentration and permeation rate are $C_m^2 = C_S^2/2$ and $j_m = i_a/2$, as given in Table 1 and as it is known from [6]. The maximum concentration C_m in permeation experiments is less than C_S because in permeation experiment only one side of the membrane is open for absorption from gas, but two sides are open for desorption. The absorption flux is divided between the re-emission and permeation fluxes, which are equal to each other if the surfaces are identical. Increase of K leads to proportional increase of both the absorption rate and the release rate; therefore C_m does not depend on K.

The situation changes in the asymmetric case. The concentration and the permeation rate can vary in wide ranges depending on the parameter of asymmetry $\gamma = K_2/K_1$. It was discussed in [7] that the permeation rate increases with increase of K_2 up to the value of the absorption rate i_a while the concentration increases up to C_S with decrease of K_2. It is useful to analyze variation of the maximum concentration and permeation rate both with K_1 and K_2 in more details. Figs. 3 and 4 show the respective dependences.

Following Eq. (10), the concentration depends on the asymmetry parameter as $(\gamma+1)^{-1/2}C_S$. Two families of normalized concentrations $C^* = C_m/Sp^{1/2}$ are plotted in Fig. 3: the first one is given as a function of K_1 at various K_2, and the second one is given as a function of K_2 at various K_1. One can see that $C_m(K_1)$ increases, and this is due to increase of the absorption rate, while $C_m(K_2)$ decreases, and this is due to promotion of the release from the outlet side. The solid and dashed curves taken at any $K_2 = K_1$ intersect at $C_m^2/S^2p = 0.5$, which is the case of the symmetric membrane. In the case of RLR, C_m equals the upper limit C_S given by Sieverts' law, where it depends neither on K_1 nor on K_2. In the opposite case of ALR, the concentration tends to be zero as $\gamma^{-1/2}C_S$ and depends both on K_1 and K_2.

The steady state permeation rate can also vary in the wide range. It is important that it can be both higher and less than in the symmetric case. Fig. 4 shows that increase of the recombination coefficient on either of the sides leads to increase of the absolute permeation rate due to increase of either absorption or recombination rate. Permeation rate $j_m(K_1)$ rises as $C_S^2K_1$ independent of K_2 in ALR and saturates at the level of $C_S^2K_2$ in RLR. Permeation rate $j_m(K_2)$ rises as $C_S^2K_2$ independent of K_1 in RLR and saturates at the level of $C_S^2K_1$ in ALR. This agrees with the approximations given in Table 1.

Table 1
Characteristic parameters of permeation in SLR

	$C^* = C_m \frac{1}{C_S}$	$\tau^* = \tau \frac{C_S}{L}$	$j^* = j_m \frac{1}{C_S^2}$	$\frac{j_m}{i_a}$
Formulas (11), (12), (14) and (15)	$\sqrt{\frac{K_1}{K_1+K_2}}$	$\sqrt{\frac{1}{K_1(K_1+K_2)}}$	$\frac{K_1K_2}{K_1+K_2}$	$\frac{K_2}{K_1+K_2}$
$K_1 = K_2 = K$	$\frac{1}{\sqrt{2}}$	$\frac{1}{K\sqrt{2}}$	$\frac{K}{2}$	$\frac{1}{2}$
ALR $K_1 \ll K_2$	$\sqrt{\frac{K_1}{K_2}}$	$\sqrt{\frac{1}{K_1K_2}}$	K_1	1
RLR $K_2 \ll K_1$	1	$\frac{1}{K_1}$	K_2	$\frac{K_2}{K_1}$

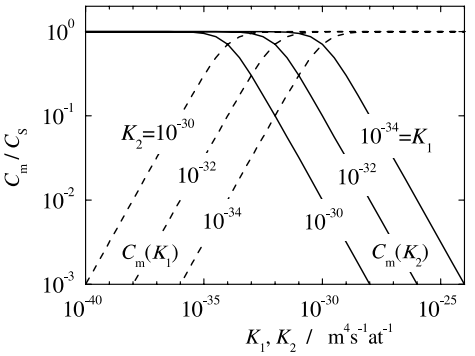

Fig. 3. Concentration normalized to Sieverts' concentration plotted as a function of the recombination coefficients. Two families are given. Solid lines are plotted as a function of K_2 at three values of K_1, dashed lines as a function of K_1 at three values of K_2.

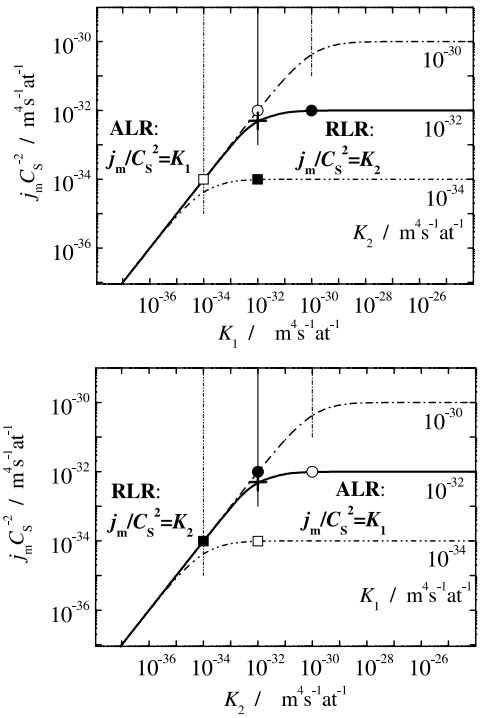

Fig. 4. Permeation rate normalized to Sieverts' concentration squared as a function of the recombination coefficient on one of the sides at different values of the recombination coefficient on another side. The vertical lines, which are drawn for $K_1 = K_2$, separate the regions of ALR and RLR for the three plots. The cross, circles and squares characterize the parameters used later in Fig. 7.

One must mention that the absolute value of the permeation rate in both modes remains proportional to the gas pressure and squared solubility as it was in the case of the symmetric SLR.

Comparing dependences of C_m and j_m on K_1 and K_2, one can find an interesting consequence: the permeation rate and the concentration can vary in different directions, so that the permeation rate can increase against decrease of the concentration.

Eq. (12) for j_m demonstrates the very important feature, which has been mentioned in [7]: the steady state permeation rate through an asymmetric membrane is symmetric with respect to K_1 and K_2. That is, it does not matter which side of the asymmetric membrane is the inlet one and which is the outlet one. In application to the experiment, this means that if one reverses the gas flow direction, applying the gas pressure from another side, the steady state permeation rate remains unchanged in SLR. This is only true in the case of pure SLR, that is if the concentration is constant over the depth.

It is interesting to analyze what part of the absorption flux is released from the back side of the membrane. One can re-write the permeation ratio j_m/i_a and the relative concentration C_m/C_S in terms of the asymmetry parameter γ as

$$j_m/i_a = \gamma/(1+\gamma) \tag{14}$$

and

$$C_m/C_S = (1+\gamma)^{-1/2}. \tag{15}$$

The dependences of C_m/C_S and j_m/i_a on the asymmetry parameter γ are shown in Fig. 5. One can see that j_m/i_a and C_m/C_S always change in the opposite directions. In RLR ($\gamma \ll 1$) the relative concentration has the maximum possible value $C_m/C_S = 1$, while only a minor part of the absorption flux permeates through the membrane: $j_m/i_a = \gamma \ll 1$. In ALR ($\gamma \gg 1$), the relative concentration tends to be zero, while almost all the particles entering the membrane permeate through its body and are released from the back side: $j_m/i_a = 1$.

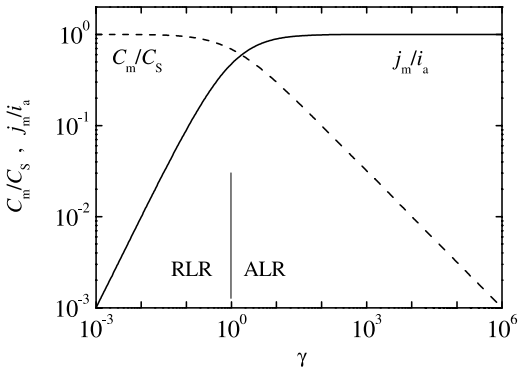

Fig. 5. The concentration normalized to Sieverts' concentration and the permeation rate normalized to the absorption flux as functions of the asymmetry parameter $\gamma = K_2/K_1$.

5. Transient features

The principal parameter, which characterizes the transient effect of permeation, is the characteristic time τ. It increases with the thickness and decreases with the pressure, and these dependences are obvious. But decrease of $\tau(S)$ seems strange from the first glance because increase of the solubility means increase of the concentration and respectively the time, which would be necessary to reach this concentration. But instead, this time decreases. The reason is that the absorption flux i_a (Eq. (9)) increases with the solubility faster than C_m (Eq. (10)). This is why τ is inversely proportional to the solubility.

The characteristic time strongly depends on surface conditions. In the case of a symmetric membrane, τ decreases with the increase of the recombination coefficient because of increase of the absorption coefficient. The characteristic time has no upper limit at low K; but at very high K, permeation is no longer surface-limited, and τ reaches its lower limit determined by diffusion.

In the asymmetric case, Eq. (11), τ decreases with increase of the recombination coefficient on either of the sides. Decrease of $\tau(K_1)$ is due to increase of the absorption flux, while decrease of $\tau(K_2)$ is due to decrease of the maximum concentration. Fig. 6 shows dependences $\tau^*(K_1)$ and $\tau^*(K_2)$, where $\tau^* = \tau C_S/L$. The limit expressions for τ^*, which are given in Table 1, are different in ALR and RLR. This is because the maximum concentrations depend on the surface conditions in different ways in the two regimes. In RLR, τ has an upper level independent of K_2 because the concentration reaches the solubility limit.

It is interesting to compare permeation through asymmetric membranes in two opposite directions, that is, the cases when we change the inlet side to the outlet one and vice versa. It was mentioned in [7] that reverse of the permeation flow does not change the maximum permeation rate but influences the characteristic time. This is illustrated in Fig. 7, which gives examples of permeation in two directions. The solid line is plotted for $K = K_1 = K_2 = 10^{-32}$ m^4 s^{-1} at^{-1}. The squares and circles are for two asymmetric membranes. One of the sides of every membrane has the recombination coefficient equal to K, while another is 100 times either higher (circles) or less (squares) than K. For both asymmetric membranes the permeation rate was calculated for two opposite directions of permeation. One can see that j_m is independent of the direction of the permeation flow, but the lag time is shorter and the permeation rate in the transient regime is higher for the case of permeation from the side with a higher recombination coefficient ($K_1 > K_2$) just because of faster absorption. In the limit case it must be $\tau_{RLR} < \tau_{ALR}$.

It is important to note that at any sets of the parameters used, the permeation rate and the characteristic

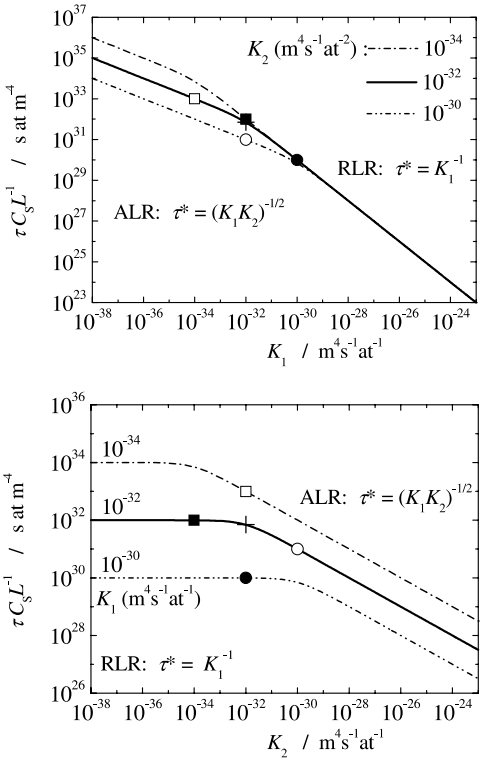

Fig. 6. The characteristic time τ (multiplied by $C_S L^{-1}$) as a function of the recombination coefficients on either the inlet or outlet side plotted for three different recombination coefficients on another side. The regions of ALR and RLR are shown. The cross, circles and squares characterize the parameters used later in Fig. 7.

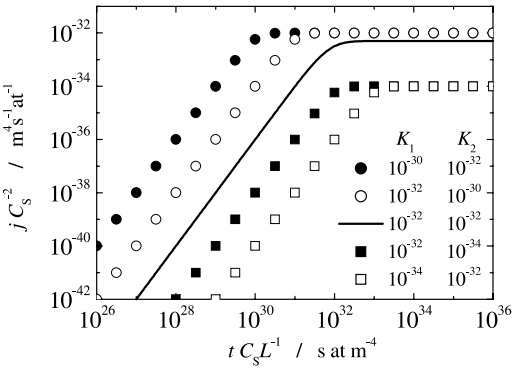

Fig. 7. Comparison of the permeation rates through the asymmetric membrane in two counter-directions (open and closed symbols) for two sets (squares and circles) of the recombination coefficients on the sides of the membrane. The line is plotted for symmetric membrane with basic value of the recombination coefficient $K = 10^{-32}$ m^4 s^{-1} at^{-1}. The values of K_1 and K_2 for asymmetric membranes are given within the figure frame. The squares and circles correspond to those in Figs. 4 and 6, and the parameters for symmetric membrane are indicated by the cross in these figures.

time change in different directions as it follows from the formula for the product $j_m\tau$. That is, increase of j_m due to any reason is always accompanied by decrease of τ, and vice versa.

6. Comparison with experiment

An analysis of an experiment made in SLR was undertaken in [7]. It was performed with Inconel 600 in the low-pressure range, which was expected to ensure SLR. It was observed that the lag time of permeation and the steady state permeation flux changed in opposite directions when changing the conditions of permeation. This agrees with predictions of the SLR model. At the same time, one must mention that the steady state permeation rate through the asymmetric membrane was different in two counter directions in those experiments. This contradicts Eqs. (5) and (13) written for SLR. The reason was possibly connected with non-zero concentration gradient in Inconel. That is, the permeation could not be characterized as that in pure SLR.

Since then, not many publications devoted to permeation in the SLR have appeared, and mostly they discuss the steady state regime. Only a few curves from literature demonstrate the dynamics of permeation. The data are often given either in relative or arbitrary units, which are not useful for the purposes of modeling. The experimental data, which can be used for comparison, were described by Yamaguchi et al. [8]. Permeation through vanadium, a material with a negative heat of hydrogen solution, was investigated. One can expect that metals with the negative heat of solution are more suitable for making the permeation experiments in SLR. The temperature was 773 K, the sample thickness 55 μm, the gas pressure 4×10^{-4} Pa. Though the permeation curve in [8] was given in relative units, one can recalculate it using the information from the paper to obtain the absolute values of the permeation rate.

One can try to describe the experimental data using various suggestions about the symmetry of permeation. It is easy to start with the case of symmetric surfaces. Two parameters, which characterize the experimental permeation plot, are j_m and τ. Using formulas for j_m and τ for the case $K_1 = K_2 = K$ from Table 1, one can obtain $K = 6.15 \times 10^{-32}$ m^4 s^{-1} at^{-1} and $S = 4.35 \times 10^{25}$ at m^{-3} Pa$^{-1/2}$. The characteristic time was taken as $\tau = 11$ min. This value of S is approximately only twice less than the value $S = 9.5 \times 10^{25}$ at m^{-3} Pa$^{-1/2}$ that can be obtained from the temperature dependence proposed in [9]. Fig. 8 shows the plot of $j(t)$ calculated with this combination of K and S and with two other characteristic times.

Fig. 8 shows also the results of calculations made in DLR. Surprisingly one can see that the curves in SLR and DLR are very similar. The diffusion coefficient used

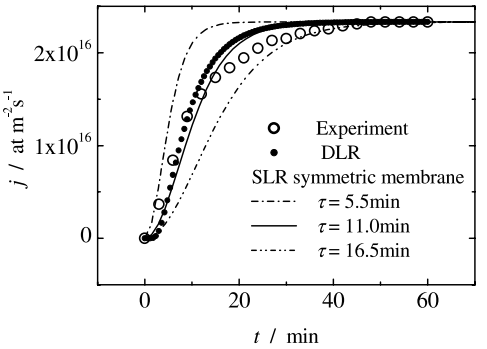

Fig. 8. Comparison of the experiment on permeation through V [8] with SLR and DLR modeling. Lines are the result of SLR modeling for a symmetric membrane for three characteristic times. Small solid circles are DLR modeling. Parameters of the experiment and calculations are in the text.

in calculations (about 7×10^{-13} m^2 s^{-1}) is several orders of magnitude less than the values available from literature (e.g. [10]). So, in the present experiments, permeation seems to be surface limited. Nevertheless, agreement of DLR with an experiment can mislead in other situations.

One can now suggest that the membrane is asymmetric, and $K_1 \gg K_2$ (RLR) as it was suggested in [8]. If to take j_m and τ to be the same in the symmetric and asymmetric cases, the formulas for RLR from Table 1 give $K_1 = 2^{1/2}K$ and $K_2 = K/2$ (the asymmetry parameter $\gamma = 2^{-3/2} = 0.354$). Fig. 9 shows a comparison of the experiment and calculations for different asymmetry parameters. The case of RLR is plotted for $\gamma = 0.354$ ($K_1 = 2^{1/2}K = 8.7 \times 10^{-32}$ m^4 s^{-1} at^{-1}, $K_2 = K/2 = 3.1 \times 10^{-32}$ m^4 s^{-1} at^{-1}) and $S = 5.05 \times 10^{25}$ at m^{-3} Pa$^{-1/2}$, which give a good agreement with the experimental steady state permeation rate. The value of solubility

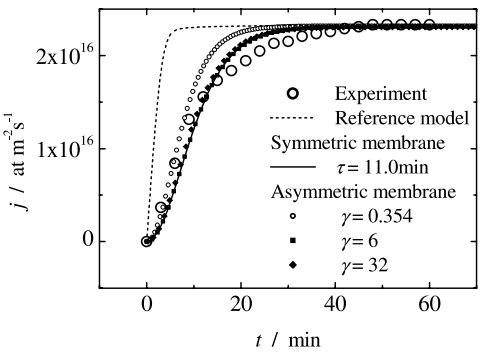

Fig. 9. Comparison of the experiment on permeation through V [8] with modeling. Dashed line is the result of modeling given in [8]. Solid line is SLR modeling with the symmetric membrane. Small circles, squares, and diamonds are SLR modeling for asymmetric membrane. Initial conditions are zero. Parameters of calculations are in the text.

used in this calculation is different from S used in symmetric case because γ is not much less than 1, and therefore the expressions for pure RLR are not exactly correct. One can see from Fig. 9 that the case of $\gamma < 1$ gives a worse agreement than the symmetric case: the permeation increases faster. Attempts to reduce γ to approach RLR conditions were negative. Indeed, $j_m\tau = LC_S\gamma$ in RLR, that is decrease of γ leads only to further decrease of τ. One can increase τ either by decreasing C_S or by decreasing K_1 Eq. (13). The former gives unacceptably low solubility value, while the latter means increase of γ, contrary to our intention to decrease it. That is, RLR (the case of $\gamma \ll 1$) is unable to suit the experiment. Fig. 9 shows also the curve from the original paper [8], which was obtained by numerical modeling using $\gamma \ll 1$; one can see that τ was very small in [8].

The opposite asymmetry $\gamma \gg 1$ (ALR) can give a better agreement. For this case, formulas of Table 1 give $K_1 = K/2$, $K_2 = 4K$, and $\gamma = 8$ if τ, j_m and C_S are taken the same as in the symmetric case. Calculations with various $\gamma \gg 1$ demonstrated that the permeation curves are close to each other and to the curve of the symmetric case. The results for $\gamma = 6$ and $\gamma = 32$ are shown in Fig. 9 as an example. The parameters for $\gamma = 6$ are $K_1 = K/2 = 3.1 \times 10^{-32}$ $m^4\,s^{-1}\,at^{-1}$, $K_2 = 3K = 1.8 \times 10^{-31}$ $m^4\,s^{-1}\,at^{-1}$, and $S = 4.7 \times 10^{25}$ $at\,m^{-3}\,Pa^{-1/2}$. Parameters for $\gamma = 32$ are $K_1 = K/8 = 7.7 \times 10^{-33}$ $m^4\,s^{-1}\,at^{-1}$, $K_2 = 4K = 2.5 \times 10^{-31}$ $m^4\,s^{-1}$ at^{-1}, and $S = 8.8 \times 10^{25}$ $at\,m^{-3}\,Pa^{-1/2}$.

One can see from this consideration that a good agreement of calculations and the experiment can be made in a very wide range of parameters. In this case, uncertainty of the parameters extracted by applying model calculations to experimental data is inevitably very high.

An analysis of the shape of the experimental curve demonstrates that it looks like the curve given in Fig. 1 for a non-zero initial condition. Therefore, the permeation rate was recalculated with $C_0 \neq 0$. Two curves are shown in Fig. 10, and agreement is good for both. The set of parameters for the curve I is: $K_1 = 2.81 \times 10^{-33}$ $m^4\,s^{-1}\,at^{-1}$, $K_2 = 1.21 \times 10^{-31}$ $m^4\,s^{-1}\,at^{-1}$, $S = 1.58 \times 10^{26}$ $at\,m^{-3}\,Pa^{-1/2}$, and $C_0 = 2 \times 10^{23}$ m^{-3}. The parameters of the curve II are: $K_1 = 7.63 \times 10^{-34}$ $m^4\,s^{-1}\,at^{-1}$, $K_2 = 7.69 \times 10^{-32}$ $m^4\,s^{-1}\,at^{-1}$, $S = 3.17 \times 10^{26}$ $at\,m^{-3}\,Pa^{-1/2}$, and $C_0 = 3 \times 10^{23}$ m^{-3}. The final steady state concentrations were calculated to be about $C_m = 2C_0$ in both cases.

These calculations show that the parameters obtained at $C_0 \neq 0$ are also uncertain. That is, non-zero initial condition brings additional problems. Calculations are very sensitive to the minor details of the shape of the permeation curve. One must have very precise experimental data to be sure about the reliability of the modeling. For the material with a negative heat of solution, absorption of residual gas prior to the experiment is very possible. As we see from the examples given, the solubilities in our calculations may differ several times while the recombination coefficients may differ two orders of magnitude, and this is not the limit.

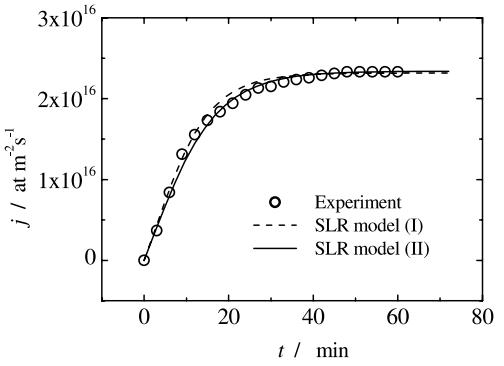

Fig. 10. Comparison of the experiment on permeation through V [8] with modeling. Two lines correspond to SLR modeling with non-zero initial conditions and different solubilities. Parameters are in the text.

One can conclude from the comparison of the model calculations and the experiment that the parameters, which are extracted, are principally uncertain. The reason is that there are only two features in the experimental curve (the lag time and the maximum permeation rate) but there are four parameters in the model (K_1, K_2, S, and C_0). The uncertainty can be reduced if to make supplementary experiments, for example on permeation in the opposite direction and on the decay of the permeation after abrupt evacuation of gas from the inlet side. In this case, the number of experimental features to be described by the model increases, and the freedom in choosing the model parameters decreases.

7. Conclusion

An analysis of gas-driven hydrogen permeation through membranes in the SLR is performed for the case of different surface conditions on the inlet and outlet sides. Analytical formula for the permeation rate as a function of time $j(t)$ has been obtained and universal time dependences of the permeation rate and the permeated quantity of gas have been demonstrated.

Variation of the maximum concentration C_m, maximum permeation rate j_m, and the characteristic time τ with variation of the surface conditions was discussed. Particularly, it was mentioned that the permeation rate increases with increase of the recombination coefficient both on the inlet side K_1 and the outlet side K_2. The characteristic time and the maximum permeation rate always change in opposite directions. The permeation rate and the concentration may change both in the same

and opposite directions, so that the permeation rate can decrease against increase of the concentration. The steady state permeation rate remains the same if the direction of the permeation flow is reversed, but the lag time is always shorter and the permeation rate in the transient mode is higher if $K_1 > K_2$ due to a higher absorption rate.

Two limit modes of SLR have been demonstrated and characterized by the asymmetry parameter $\gamma = K_2/K_1$. The ALR takes place at $\gamma \gg 1$ and the RLR at $\gamma \ll 1$. Expressions for C_m, j_m, and τ have been obtained in the limits of ALR and RLR.

Features of the permeation curves are different in the two modes. In RLR, the permeation rate is much less than the absorption flux i_a, while the concentration reaches its maximum available value C_S determined by Sieverts' law. In ALR, the permeation rate practically equals the absorption rate and does not depend on γ, while the concentration becomes very low. In general, $j_m(\gamma)/i_a$ increases while $C_m(\gamma)$ decreases.

Comparison of the model with experimental data on deuterium permeation through vanadium available from literature has been made. The model gives rather good agreement with the experiment with zero initial concentration; modeling with non-zero concentration gives a very good agreement with the experiment.

It has been demonstrated that parameters, which can be extracted from measurements of the permeation rate, are very uncertain in principal. Good fitting can even be made assuming both $\gamma < 1$ and $\gamma > 1$. Besides, it has been demonstrated that non-zero initial conditions could be a very serious factor, which reduces the reliability of modeling in SLR. The recombination coefficients obtained from the same permeation curve can differ by orders of magnitude. Measurements of the accumulation curves instead of permeation curves can seriously mislead in interpretation of the experiment if non-zero conditions are possible, as decrease of lag time down to the values typical for DLR is possible.

Additional experiments on permeation in two opposite directions and measurements of the permeation decay after gas supply termination can increase the reliability of data obtained by the membrane permeation technique.

References

[1] O.W. Richardson, J. Nicol, T. Parnel, Philos. Mag. 8 (1904) 1.
[2] H. Daynes, Proc. Roy. Soc. A 97 (1920) 286.
[3] C. Wagner, Z. Physikal. Chem. A 159 (1932) 459.
[4] J. Wang, Proc. Cambridge Phil. Soc. 32 (1936) 657.
[5] A. Livshits, Z. Tekhnicheskoi Fiziki 47 (1977) 1559.
[6] I. Ali-Khan, K.J. Dietz, F.G. Waelbroeck, P. Wienhold, J. Nucl. Mater. 76&77 (1978) 337.
[7] F. Waelbroeck, P. Wienhold, J. Winter, E. Rota, T. Banno, Influence of bulk and surface phenomena on the hydrogen permeation through metals, KFA Jülich Report Jül-1966, Jülich, Germany, 1984.
[8] K. Yamaguchi, S. Tanaka, M. Yamawaki, J. Nucl. Mater. 179–181 (1991) 325.
[9] E. Velekis, R.K. Edvards, J. Phys. Chem. 73 (1969) 683.
[10] D.T. Peterson, B.J. Schlader, Metall. Trans. A 19A (1988) 67.